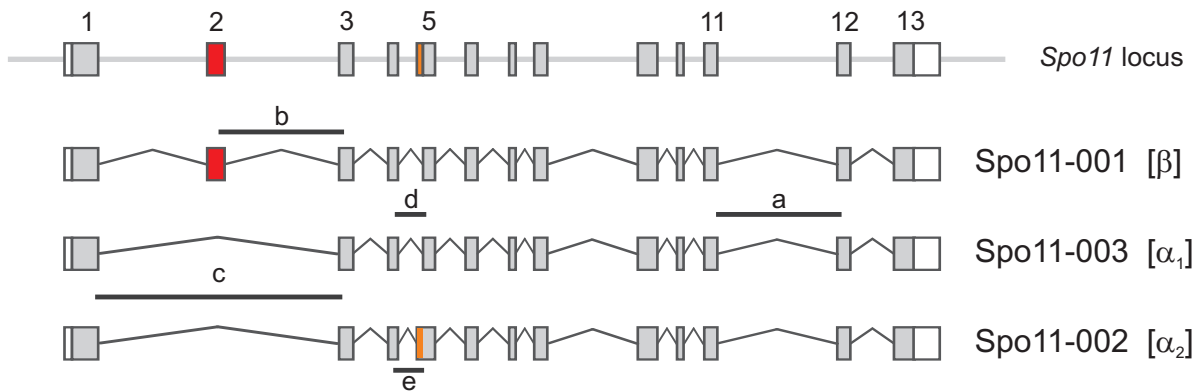


Sup. Figure 1

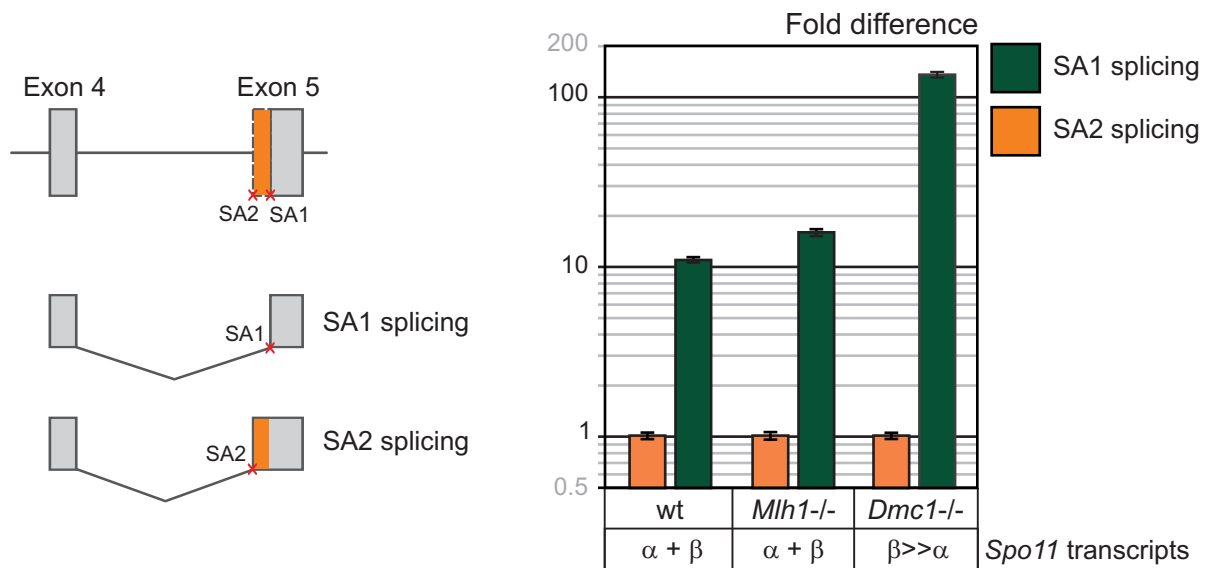
A



Taqman assay

a	targets Exon 11-12 junction	Detects all <i>Spo11</i> transcripts
b	targets Exon 2-3 junction	Detects <i>Spo11</i> β transcripts
c	targets Exon 1-3 junction	Detects <i>Spo11</i> α transcripts [both α_1 and α_2]
d	targets Exon 4-5 junction, using 3'ss SA1	
e	targets Exon 4-5 junction, using 3'ss SA2	

B



SA1 => [LILKVLSMIYKLIQSDTYATKRDIY](#)**Y**TDSQLFGNQAAVDSAIDDISCMLKVPRRSLHV

SA2 => [LILKVLSMIYKLIQSDTYATK](#)**RSNAHSVLTLLH**LRDIY**Y**TDSQLFGNQAAVDSAIDDISCMLKVPRRSLHV

Exon 4

encoded by Exon 5

[A] Mouse *Spo11* locus scheme and alternative mRNA transcripts as annotated in Ensembl genome database. a, b and c indicate the exon junctions targeted by the different Taqman assays used to quantify total and isoform-specific *Spo11* transcripts. d and e were designed to detect two alternative exon 4-5 junctions resulting from the use of the alternative 3' splice acceptors in intron 4.

[B] In the exon 4-5 boundary, SA1 splicing events are 10 times more frequent than SA2 splicing events: The relative abundance of SA1 and SA2 splicing products in wild type, *Mlh1*^{-/-} and *Dmc1*^{-/-} testicular RNA was determined by RT-qPCR, using the Taqman assays (d and e) described in [A].

Sup. Fig. 1: the 39.7 KDa band corresponds to a SPO11 α minor splicing isoform.

The minor bands observed in wild type testis extracts (indicated by * and ** in **Fig. 4A**) could represent minor splicing isoforms of SPO11 α/β or post-translationally modified SPO11 α isoforms. There is no difference in the band pattern of anti-SPO11 immunoprecipitates, either when treating them with phosphatases (λ phosphatase or protein phosphatase 1), or when including phosphatase inhibitors in buffers during lysis and immunoprecipitation (data not shown). Thus we ruled out the possibility that these minor bands might correspond to phosphorylated SPO11 α .

Ensembl annotation describes a second SPO11 α isoform (SPO11-002) generated by the use of an alternative 3' splice acceptor at the exon 4-5 boundary, that includes thirty nine extra nucleotides in exon five, leading to the addition of thirteen extra amino acids [RSNAHSVLTLHLH] to the polypeptide (**Sup. Fig. 1A**). This third isoform is expected to have a molecular weight of 41.8 KDa, and migrate slightly slower than the SPO11 α isoform [40.3 KDa] (See **Fig. 4C**). Hence, it could be consistent with the faster migrating minor band we observe in wild type extracts, estimated to have a mass 1.5 KDa greater than that of SPO11 α (marked with * in **Fig. 4A**). We designed two Taqman assays that can specifically detect either of the two alternative junctions between exons four and five (**Sup. Fig. 1AB**, assays d and e), in order to examine the presence of these alternatively spliced transcripts in wild type and mutant testes.

In the wild type and *Mlh1*^{-/-} samples, roughly one out of ten splicing events between exons four and five resulted in incorporation of the extra nucleotides to exon five, indicating that this alternative splice acceptor is used less frequently and creates a quantitatively minor isoform (**Sup. Fig. 1B**). In the *Dmc1*^{-/-} mutant, which carries almost exclusively *Spo11* β transcripts, only one out of one hundred events led to the alternative splicing variant including the extra nucleotides (**Sup. Fig. 1B**). This confirms that the use of this alternative splice acceptor (SA₂) occurs primarily on α transcripts, as reported in the Ensembl annotation. All together, these data suggest that there is a minor fraction of α transcripts carrying the extra nucleotides that would result in a SPO11 α polypeptide with a slightly higher molecular weight. Therefore it would be consistent with the minor, slower migrating band seen just above SPO11 α in wild type and *Mlh1*^{-/-} testis extracts in our westerns (* in **Fig. 4A**).

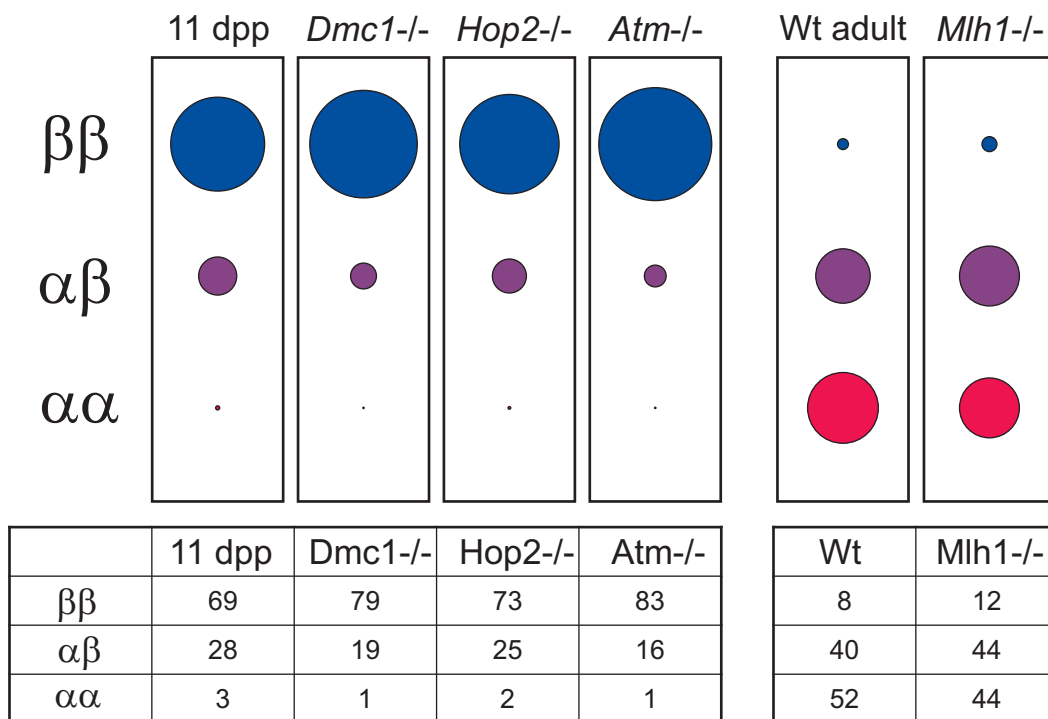
We are still uncertain as to the identity of the second minor band (41.2 KDa, marked by ** in **Fig. 4A**), except for the observation that both minor bands are detected only when SPO11 α is present and above a certain threshold (**Fig. 4DE**). They are not detected in *Dmc1*^{-/-}, *Hop2*^{-/-} and *Atm*^{-/-} extracts, in which we detect primarily SPO11 β , suggesting that the 41.2 KDa band is another minor splicing isoform of SPO11 α .

Sup. Figure 2

A $\alpha:\beta$ ratio in the different samples

	11 dpp	Dmc1-/-	Hop2-/-	Atm-/-	Wt	Mlh1-/-
α	1	1	1	1	2.6	2
β	5	8	6	10	1	1

B Probability of forming $\alpha\alpha$ $\alpha\beta$ $\beta\beta$ dimers given the $\alpha:\beta$ ratio



Supplementary Figure 2: measured $\alpha:\beta$ polypeptide ratio and estimated proportion of homo ($\alpha\alpha$, $\beta\beta$) and hetero ($\alpha\beta$) dimers formed in wild type and mutant mice testes.

[A] $\alpha:\beta$ polypeptide ratio: calculated from relative intensities of the α and β bands in Ip/WB with anti-SPO11 antibody in wild type and several mutant mice (from figure 3DE).

[B] Estimated probability of forming $\alpha\alpha$, $\alpha\beta$, $\beta\beta$ dimers, given the measured $\alpha:\beta$ polypeptide ratio: Judging by sequence alignment of SPO11 with Topo VIA, all residues predicted to be involved in the monomer-monomer interphase in a dimer are downstream of the region encoded by exon 2 and therefore common to both isoforms, so we think it is correct to assume that there is no bias towards either homo or hetero dimer formation. Thus, on the basis of the measured $\alpha:\beta$ polypeptide ratio, it is possible to calculate the probability of formation of the different kinds of dimers as follows:

If $\alpha/\beta = a/b$ and $a+b=c$

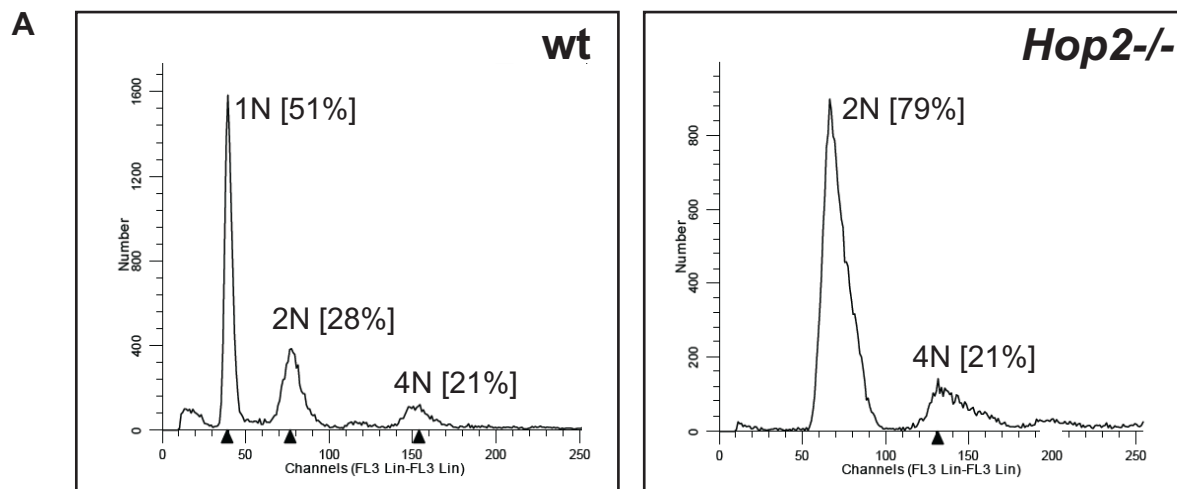
Probability of $\alpha\alpha$ dimer = $a/c \times a/c$

Probability of $\beta\beta$ dimer = $b/c \times b/c$

Probability of $\alpha\beta$ dimer = $(a/c \times b/c) + (b/c \times a/c)$

The table summarizes the estimated probability of the different kinds of dimers given the $\alpha:\beta$ ratio shown in [A] for 11 dpp wild type pups, the different mutants and wild type adult mice. In the bubble graph, the diameter of each circle is proportional to the fraction of total dimers represented by each kind of dimer.

Sup. Figure 3



Testicular cells	wt	<i>Hop2</i> ^{-/-}
Total	1.2 x 10 ⁷	2.1 x 10 ⁶
% Viable	98.7 %	98%
1N	51%	ND
2N	28%	79%
4N	21%	21%

B *Hop2*^{-/-} spreads counts.

Other		771	73%	
pre-Leptotene		88	8%	
prophase I	Leptotene	52	19%	26%
	Zygotene/Pachytene	147		74%
Total		1058	100%	100%

Supplementary Figure 3: Determining the proportion of primary spermatocytes and leptotene spermatocytes in *Hop2*^{-/-} testes.

[A] Determining the proportion of primary spermatocytes in wt and *Hop2*^{-/-} testes: testicular cell suspensions were fixed, stained with PI and analyzed by flow cytometry on the basis of their DNA content. We determined the proportion of primary spermatocytes based on their characteristic 4N DNA content.

[B] Determining the proportion of primary spermatocytes corresponding to leptotene spermatocytes in *Hop2*^{-/-} spermatocytes: *Hop2*^{-/-} chromosome spreads were stained with DAPI and antibodies against SCP3 and γ H2AX. Over 1000 cells were scored and classified as pre-leptotene, leptotene, zygote/pachytene spermatocytes, and other (spermatogonia + other mitotic cells), based on the immunostaining and DAPI nuclear pattern.